Rhein exerts anti-multidrug resistance in acute myeloid leukemia via targeting FTO to inhibit AKT/mTOR

Shuling Zhang[a], Lanxia Zhou[b], Jincai Yang[a], Jianle Lu[a], Lili Tao[a], Youfan Feng[a], Juan Cheng[c] and Li Zhao[b]

Chemotherapy failure and resistance are the leading causes of mortality in patients with acute myeloid leukemia (AML). However, the role of m6A demethylase FTO and its inhibitor rhein in AML and AML drug resistance is unclear. Therefore, this study aimed to investigate the antileukemic effect of rhein on AML and explore its potential mechanisms underlying drug resistance. Bone marrow fluid was collected to assess FTO expression in AML. The Cell Counting Kit 8 reagent was used to assess cell viability. Migration assays were conducted to assess the cell migration capacity. Flow cytometry was used to determine the apoptotic effects of rhein and western blot analysis was used to detect protein expression. Online SynergyFinder software was used to calculate the drug synergy scores. The in-vivo antileukemic effect of rhein was assessed in an AML xenograft mouse model. We analyzed different types of AML bone marrow specimens to confirm that FTO is overexpressed in AML, particularly in cases of multidrug resistance. Subsequently, we conducted in-vivo and in-vitro investigations to explore the pharmacological activity and mechanism of rhein in AML and AML with multidrug resistance. The findings demonstrated that rhein effectively suppressed the proliferation and migration of AML cells in a time- and dose-dependent manner and induced apoptosis. Rhein targets FTO, inhibits the AKT/mTOR pathway, and exhibits synergistic antitumor effects when combined with azacitidine. This study elucidates the significant role of FTO and its inhibitor rhein in AML and AML with multidrug resistance, providing new insights for overcoming multidrug resistance in AML. ***Anti-Cancer Drugs*** **35: 597–605**

Anti-Cancer Drugs 2024, **35**:597–605

Keywords: acute myeloid leukemia, AKT/mTOR, FTO, multidrug resistance, rhein

[a]The First Clinical Medical College, Lanzhou University, [b]Clinical Cellular Molecular Genetics and Immunology Laboratory and [c]Department of Hematology, The First Affiliated Hospital of Lanzhou University, Lanzhou, China

Correspondence to Li Zhao, MD, Clinical Cellular Molecular Genetics and Immunology Laboratory, The First Affiliated Hospital of Lanzhou University, Lanzhou 730013, China
Tel: +86 182 9833 4160; e-mail: zhaoli@lzu.edu.cn

Received 7 March 2024 **Revised form accepted** 8 March 2024.

Introduction

Acute myeloid leukemia (AML) is a heterogeneous group of primary hematopoietic neoplasms that primarily arise from cells committed to the myeloid lineage. The Surveillance, Epidemiology, and End Results database reported approximately 61 090 diagnosed cases of leukemia in 2021, ranking it the tenth most common cancer in the United States. Among these cases, the incidence of AML is the highest and has steadily increasing over the years. AML has a high incidence rate in the elderly population [1]. Despite significant advancements in AML treatment, relapse and multidrug resistance persist as primary causes of mortality [2]. Ongoing research on AML drug resistance predominantly centers on drug-binding site mutations, overexpression of drug efflux pumps, alterations in biological metabolism, and disruption of cell signaling pathways. Evidence, however, indicates that epigenetic modifications, particularly N^6-methyladenosine (m^6A), also plays an important role in AML drug resistance [3–6]. m^6A is the most prevalent and abundant internal modification in mRNAs and plays an essential role in regulating mRNA metabolism and fate, including stability, translation, splicing, and transport. The dynamic and reversible m^6A modification is regulated by specific enzymes, known as 'writers' (METTL3, METTL14, WTAP), 'readers' (YTHDF1/2/3, YTHDC1/2, IGF2BP1/2/3), and 'erasers' (fat mass and obesity-associated [FTO] and ALKBH5) [7]. FTO, the first discovered m^6A demethylase, plays a vital role in cancer cell proliferation, apoptosis, cell cycle, migration, invasion, and drug resistance, can remove m^6A methylation from RRACH motifs in mRNAs and lncRNAs within cells [8,9]. FTO upregulation often promotes AML. It regulates the target genes ASB2 and RARA and reduces m^6A levels in these mRNA transcripts, thereby enhancing leukemia oncogene-mediated cell transformation and leukemogenesis, while inhibiting AML cell differentiation [10].

Rhein (4,5-dihydroxyanthraquinone-2-carboxylic acid) is a natural anthraquinone derivative that is predominantly found in the rhizome of the well-known traditional Chinese herb rhubarb. It exhibits multiple pharmacological activities, including anticancer, anti-inflammatory, and anti-angiogenic properties [8]. Rhein was discovered by Chen *et al.*'s team as the first small-molecule inhibitor

 DOI: 10.1097/CAD.0000000000001608

of FTO. It competitively binds to the FTO active site and significantly inhibits m^6A demethylation in cells [9]. Increasing evidence from numerous studies indicates that rhein exhibits antitumor effects in various types of cancers, such as ovarian, liver, and pancreatic cancer [11–13].

In this study, we discovered that rhein induced AML cell apoptosis and inhibited proliferation and migration by targeting FTO and protein kinase B/mammalian target of rapamycin (AKT/mTOR) pathways. For the first time, we demonstrated the involvement of rhein in AML multidrug resistance and its synergistic antitumor effect with DNA demethylation drugs. Targeting FTO as a therapeutic approach holds promise as a novel strategy for future clinical treatments, and rhein, as a small molecule inhibitor, represents a potential new anticancer drug for AML treatment and overcoming multidrug resistance.

Materials and methods

Extraction of acute myeloid leukemia bone marrow mononuclear cells

Bone marrow samples were collected from normal bone marrow transplant donors, as well as from patients with primary AML, complete remission after chemotherapy, and relapsed/refractory AML. Informed consent was obtained from all the patients. Mononuclear cells were isolated using density gradient centrifugation. Fresh bone marrow fluid was carefully aspirated using a pipette and added slowly along the tube wall into a 15 ml centrifuge tube containing 3 ml of lymphocyte separation solution. The tube was then centrifuged at 600 g for 30 min to obtain the separation solution, which formed four distinct layers: a plasma layer, ring-shaped milky white mononuclear cell layer, a transparent separation fluid layer, and red blood cell layer. The mononuclear cell layer was transferred to another 15 ml tube using a pipette, and 10 ml of PBS solution was added. The tube was centrifuged at 200 g for 10 min. This process was repeated twice to obtain a final pellet of AML bone marrow mononuclear cells.

Cell lines and cell culture

The AML cell lines MV4-11 and MOLM-13 were purchased from ATCC, USA. HL60, THP1, the human adriamycin-resistant AML cell line HL60-adriamycin (ADR) were purchased from Winter Biotechnology, China. K562 and the human adriamycin-resistant AML cell line K562-ADM were obtained from the Central Laboratory of the First Hospital of Lanzhou University, China. OCI-AML3 was purchased from Fu Heng Biology, China. THP1 and OCI-AML3 cells were cultured in Roswell Park Memorial Institute medium (RPMI) 1640 medium (Gibco, USA) supplemented with 15% fetal bovine serum (Excell Bio, China), and 1% penicillin-streptomycin (Solarbio Life Sciences, China), whereas the other cells were cultured in RPMI 1640 medium supplemented with 10% fetal bovine serum and 1% penicillin–streptomycin. All the cells were maintained in a humidified incubator at 37 °C with 5% CO_2.

Protein extraction and western blot analysis

The cells were collected and washed twice with precooled PBS, RIPA buffer (Beyotime, China) containing protease inhibitors and phosphatase inhibitor was added, and the mixture was vortexed and placed on ice for 20 min for lysis. After centrifugation at 14 000*g* for 15 min, the supernatant was collected, and the protein concentration was determined using a BCA protein assay kit (Solarbio Life Sciences). Twenty microgram of protein was loaded onto a 10% SDS-PAGE gel (NCM Biotechnology, China) for electrophoresis, and then transferred the separated protein to a PVDF membrane (Merck Millipore Company, Germany). The membranes were blocked with 5% skim milk powder and incubated with the primary antibody at 4 °C overnight. The membrane was washed with tris-buffered saline tween-20 and incubate with secondary antibody for 1 h at room temperature. The color was developed with enhanced chemiluminescence chemical chromogenic solution and photographed using a chemiluminescence imaging system (Amersham Imager 680).

Cell proliferation assay

Rhein (purchased from MCE Company, USA) was dissolved in dimethyl sulfoxide (DMSO) and prepared at a concentration of 40 mM through sonication and heat treatment to promote dissolution. The solution was then stored at −20 °C. Cells were seeded in 96-well plates (NEST, Wuxi NEST Life Science & Technology Co) at a density of 2×10^4 cells/well and treated with varying doses of rhein. HL60 and K562 cells were exposed to rhein at concentrations of 0, 10, 20, 50, 100, and 200 μM, while adriamycin-resistant cell lines K562-ADM and HL60-ADM were treated with 0, 10, 20, 50, 100, 200, and 400 μM. Subsequently, 10 μl of Cell Counting Kit 8 reagent (CCK8) from NCM Biotechnology was added to each well at 24, 48, 72 h and prevent bubble formation, and the absorbance was measured at 450 nm using a microplate reader after incubation at 37 °C for 3 h. Azacitidine (AZA) was purchased from MCE Company, dissolved in DMSO to prepare a stock solution with a concentration of 100 mM, and stored at −20 °C. HL60 and HL60-ADR cells were seeded in a 96-well plate at a density of 2×10^4 cells/well and treated with different doses of AZA. After 48 h, 10 μL of CCK8 was added to each well and incubated at 37 °C for 3 h. The absorbance was then measured at 450. Subsequent experiments will determine the drug concentration gradient based on the IC50 values.

Flow cytometric analysis

Following treatment with rhein at varying concentrations (0, 50, 100 μM) for 48 h, a total of 5×10^5 cells were

collected and suspended in 500 µl of 1× binding buffer. For staining, V-APC (5 µl) and 7-AAD (10 µl) were added to each tube and vortexed gently to ensure proper mixing. The cells were then incubated in the dark for 5 min and subsequently analyzed using a BD FACS (Becton, Dickinson and Company, USA) Verse flow cytometer. The obtained results were analyzed using the NovoExpress software.

Transwell cell migration assay

Migration experiments were performed using an 8 µm aperture 24-well transwell chamber (NEST). HL60 and HL60-ADR cells were treated with different rhein concentrations (0, 50, 100 µM) for 24 h. The cells were collected, counted, and suspended in serum-free RPMI 1640 medium. The upper chamber of the transwell was seeded at a density of 2×10^6 cells/well, whereas the lower chamber was filled with 600 µl of culture medium containing 10% foetal bovine serum. After 24 h of incubation, the transwell chamber was washed twice with PBS, fixed with 4% paraformaldehyde for 15 min, and stained with 0.1% crystal violet for 20 min. Non-migrated cells in the upper chamber were carefully removed using a cotton swab. The migrated cells at the bottom of the upper chamber were observed under a microscope, and five random areas were photographed. The number of migrating cells was quantified using Image J software (National Institutes ofHealth, USA), and the absorbance value of the cells migrating to the lower chamber was detected using CCK8.

Synergy determination with SynergyFinder

HL60 and HL60-ADR cells were seeded into 96-well plates at a density of 2×10^4 cells per well and treated with single drugs (AZA, rhein) and combination drugs (AZA and rhein), based on their respective IC50 values from the cytotoxicity assay. Cell viability was assessed at a constant dilution ratio of the two inhibitors: rhein concentrations (10, 20, 40, and 80 µM) and AZA concentrations for HL60 (0.062, 0.125, 0.25, and 0.5 µM) and HL60-ADR (10, 100, 200, and 500 µM). After 48 h of treatment, cell viability was measured using a CCK-8 Kit and a plate reader. The online SynergyFinder software Amersham Imager 680, Ultrasensitive Multifunctional Imager (Cellular Technology, USA) (https://synergyfinder.fimm.fi) was used to calculate drug synergy scores using the response surface model and zero interaction potency (ZIP) calculation method. Drug combinations with ZIP Synergy scores greater than 0 were considered synergistic (red regions) [14,15]. Heat maps were generated based on response patterns to evaluate the therapeutic significance of the drug combinations.

Xenograft model

Female no obesity diabetes-severe combined immune deficiency mice, aged 4 weeks, were obtained from GemPharmatech Co., Ltd., China. After one week of acclimatization, the mice were randomly allocated into four groups with five mice in each group: HL60, HL60+rhein, HL60-ADR, and HL60-ADR+rhein. A subcutaneous injection of 1×10^7 cells was performed near the front armpit of the mice after disinfection with alcohol. The growth of the transplanted tumors and the condition of the mice were assessed daily. Visible tumors were measured using a Vernier caliper the following day. Tumor growth was evaluated by calculating tumor volume using the formula $V = (\text{length} \times \text{width}^2)/2$. Upon reaching an average tumor volume of approximately 100 mm^3, rhein was administered intraperitoneally to the HL60+rhein and HL60-ADR+rhein groups at a dose of 20 mg/kg/day, while the control group received an equivalent dose of saline. After 2 weeks of drug treatment, the mice were euthanized, dissected, and the tumor size was measured. The Ethics Committee of the First Hospital of Lanzhou University approved all the animal experiments.

Statistical analyses

Data analysis was performed using the GraphPad Prism software (version 8.0). The results are reported as mean ± SD, and statistical significance was assessed using nonlinear regression or one-way analysis of variance. A standard *t*-test was used to assess the differences between two groups. All experiments were conducted at least three times. Statistical significance was defined as a *P*-value less than 0.05, with levels of significance annotated as follows: $^{****}P < 0.0001$, $^{***}P < 0.001$, $^{**}P < 0.01$, and $^{*}P < 0.05$.

Results

High expression of FTO is associated with drug resistance in acute myeloid leukemia

Our findings demonstrate that FTO expression is elevated in AML patients compared to normal donors, with particularly high expression observed in relapsed/refractory AML patients. Additionally, FTO expression was diminished in complete remission patients when compared to that in primary AML patients (Fig. 1a). AML cell lines, including THP1, HL60, MV4-11, MOLM13, OCI-AML3, and K562, exhibited increased FTO expression compared to normal donors. Additionally, we observed a significant increase in FTO expression in the drug-resistant cell line HL60-ADR/K562-ADM compared to that in HL60/K562 cells. Moreover, we verified overexpression of the multidrug resistance protein ABCB1 in drug-resistant strains (Fig. 1a).

Rhein inhibits the proliferation and induces apoptosis in acute myeloid leukemia

After AML cells were treated with different concentrations of rhein, the viability of AML cells decreased with an increase in drug dose and the prolongation of drug action time(Fig. 1b), demonstrating that the inhibitory

Fig. 1

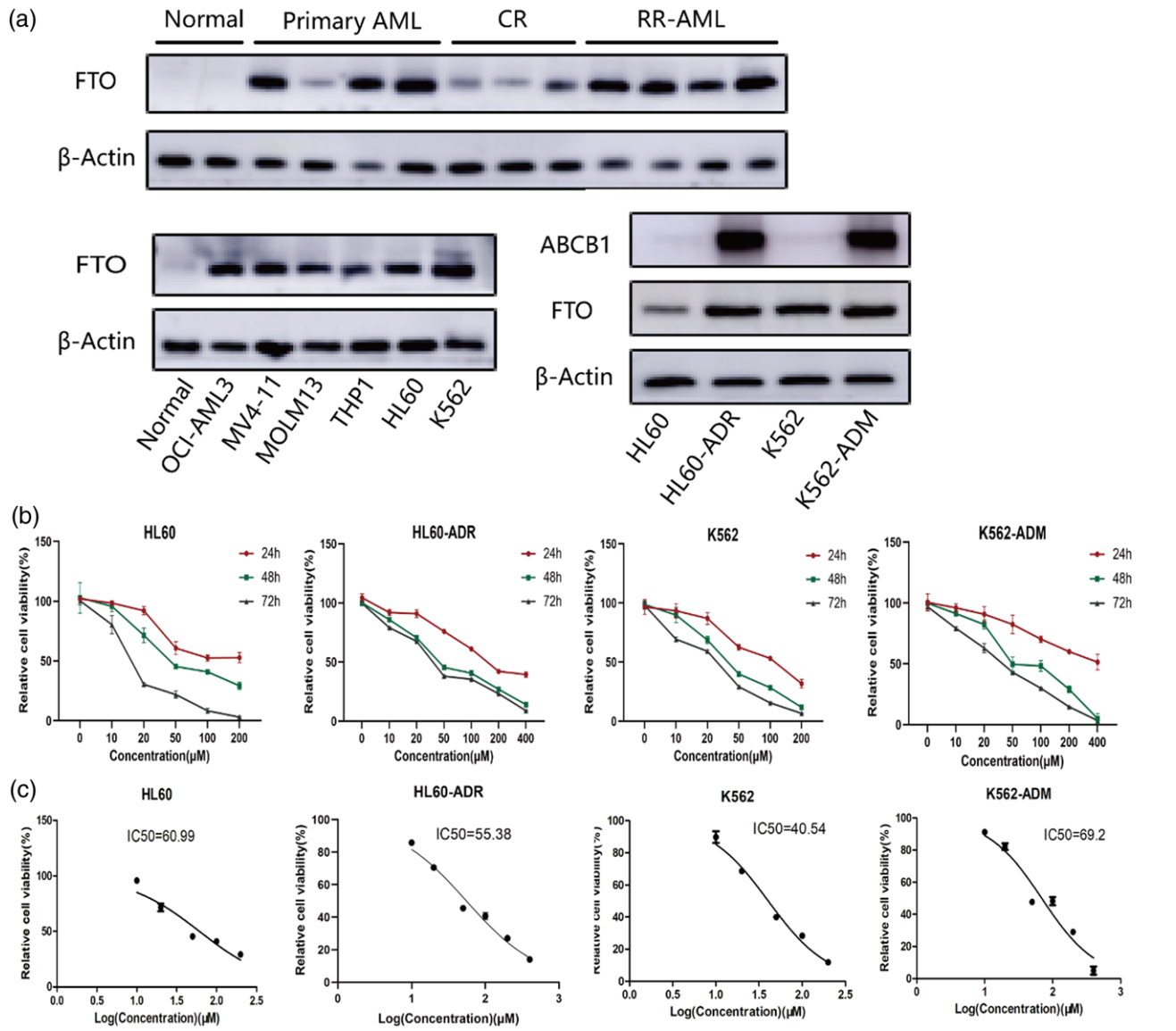

Expression of FTO in AML and rhein inhibits AML cell proliferation. (a) Expression of FTO in AML patients and AML cell lines. (b) Viability of AML cells treated with different concentrations of rhein. (c) IC50 value of AML cells treated with rhein for 48 h. CR, complete remission after chemotherapy; FTO, fat mass and obesity-associated; RR-AML, relapsed and refractory AML.

effect of rhein on the proliferation of AML cells is dose- and time-dependent. Furthermore, the IC50 values of rhein are close in HL60 (IC50 = 60.99 μM)/K562 (IC50 = 40.54 μM), and HL60-ADR (IC50 = 55.38 μM)/ K562-ADM (IC50 = 69.2 μM), suggesting that rhein exhibits comparable inhibitory effects on cell proliferation in AML parent cells and drug-resistant cells(Fig. 1c). Flow cytometry analysis revealed that rhein effectively induced apoptosis in AML cells in a dose-dependent manner, with higher concentrations of rhein leading to greater apoptosis rates in both HL60 and HL60-ADR cells (Fig. 2a and b). Additionally, western blot analysis showed that rhein treatment significantly decreased the expression of Bcl-2 protein in both HL60 and HL60-ADR cells, while increasing BCL2 associated X protein expression after a 48-hour treatment (Fig. 2c).

Rhein inhibits acute myeloid leukemia migration

The migratory ability of AML cells greatly increases the occurrence of extramedullary infiltration, which is associated with disease recurrence and a poor prognosis. In order to evaluate the effect of rhein on the migration ability of AML cells, we treated HL60 and HL60-ADR cells with different concentrations of rhein for 24 h, then

Fig. 2

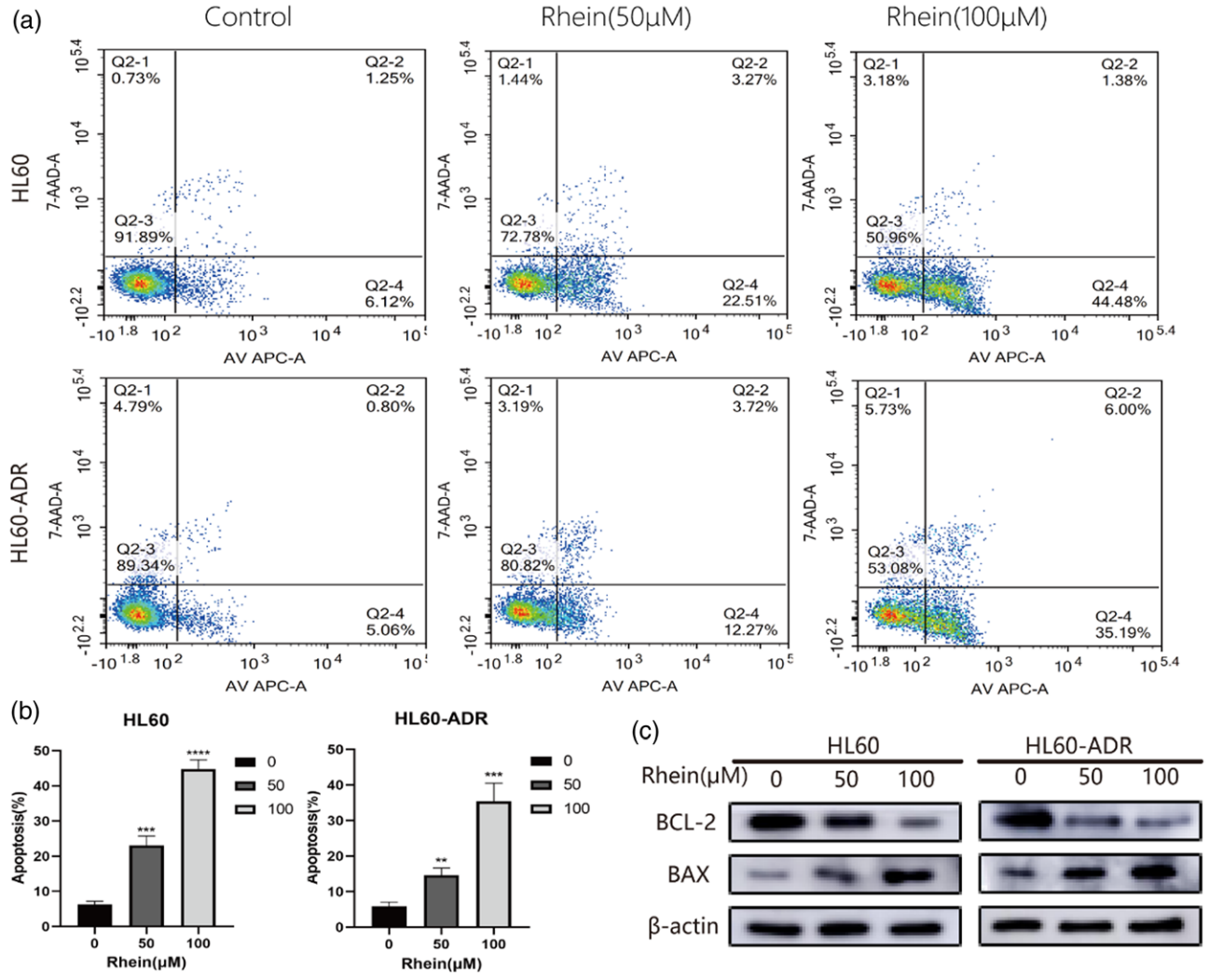

Rhein induces apoptosis in AML: (a and b) flow cytometry to detect the proapoptotic effect of rhein (0, 50, and 100 μM) on HL60 and HL60-ADR cells; (c) WB to detect the effect of rhein on the expression of BCL-2 and BAX. AML, acute myeloid leukemia; BAX, BCL2 associated X protein; WB, western blot.

centrifuged to remove the drug and performed a Transwell experiment. The number of cells on the upper chamber membrane decreased in the rhein-treated group, as did the number of cells in the lower chamber. Analysis of the cells collected from the lower chamber and measurement of the optical density (OD) revealed a lower OD value in the rhein-treated group than in the blank group (Fig. 3a–d). Our study provides evidence for the significant inhibitory effect of rhein on AML cell migration. Moreover, we observed a dose-dependent decrease in the number of migrating cells as the rhein concentration increased.

Rhein inhibits the AKT/mTOR pathway

After treating cells with various concentrations of rhein, western blot analysis revealed that rhein effectively suppressed the expression of FTO protein in a concentration-dependent manner. Previous studies have demonstrated that rhein exhibits potent antitumor effects by modulating the AKT/mTOR pathway in various types of tumors [16,17]. In HL60 and HL60-ADR cells, the total expression of AKT and mTOR molecules did no differ as the concentration of rhein increased, however, the expression levels of phosphorylated AKT and phosphorylated mTOR gradually decreased, indicating that rhein significantly inhibited the activity of the AKT/mTOR pathway. Subsequent analysis of the pathway' activity in both AML parental strains and drug-resistant strains revealed increased expression of phosphorylated mTOR in the drug-resistant strains (Fig. 3e).

Synergistic antileukemic effects of rhein and azacitidine

Our study confirmed that HL60-ADR exhibits multidrug resistance. The IC50 of AZA for HL60 cells was

Fig. 3

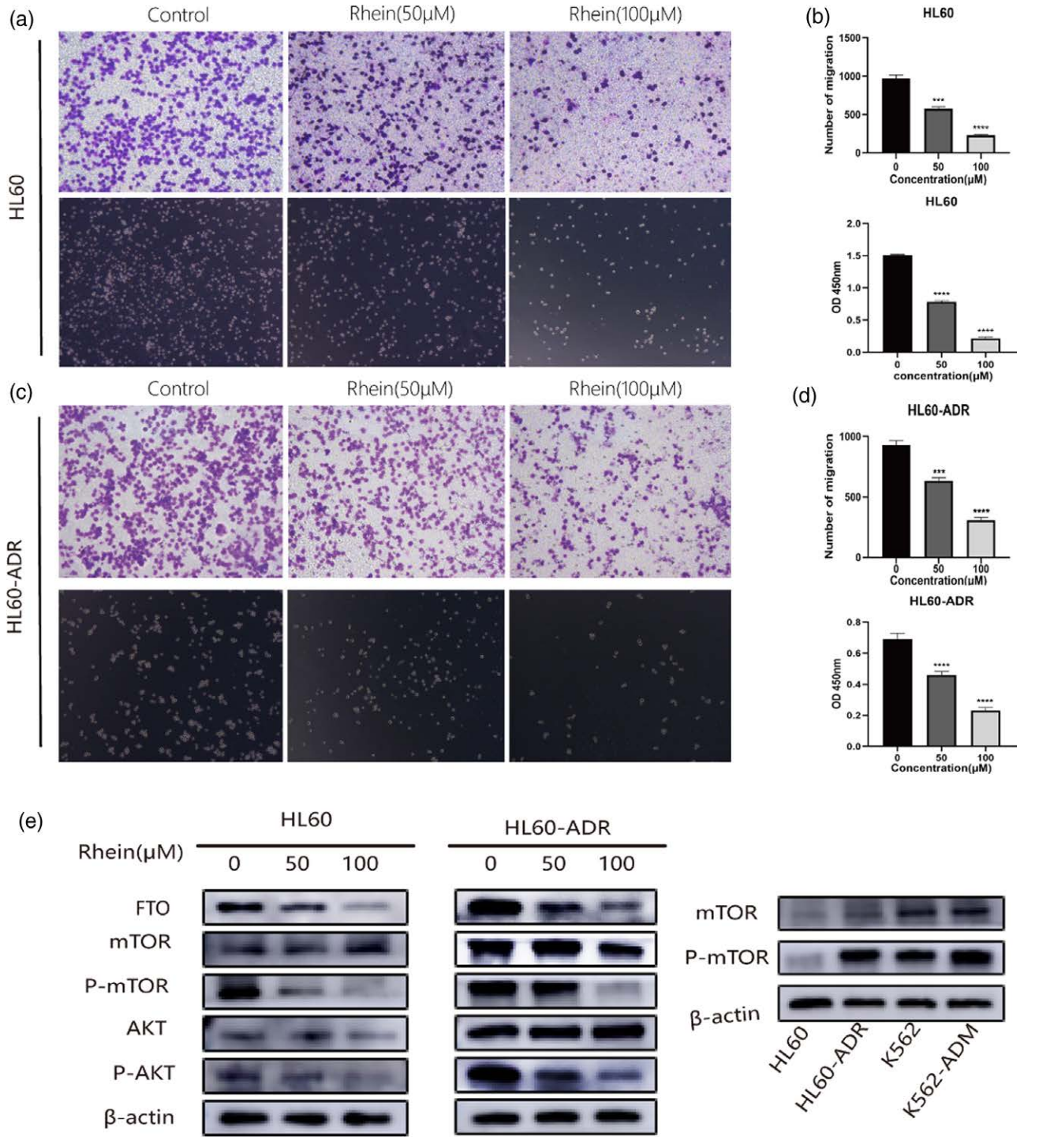

Rhein inhibits AML cell migration and AKT/mTOR pathway: (a and c) Migration of HL60 and HL60-ADR after treatment of cells with different concentrations (0, 50, and 100 μM) of rhein for 24 h. (b and d) The number of cells migrating to the under-side of up chamber membrane and absorbance values detected by CCK8 for cells falling into the lower chamber. (e) Rhein suppresses AKT/mTOR pathway and expression of mTOR pathway is higher when AML with drug-resistant. ADR, adriamycin; AKT/mTOR, protein kinase B/mammalian target of rapamycin.

0.9764 μM, whereas HL60-ADR displayed an IC50 of 385 μM (Fig. 4a). HL60-ADR exhibited approximately 400-fold resistance to AZA compared to HL60, suggesting that it is resistant to both ADR and AZA. This observation supports the notion that AML drug-resistant cells exhibit multidrug resistance, along with elevated expression of

Fig. 4

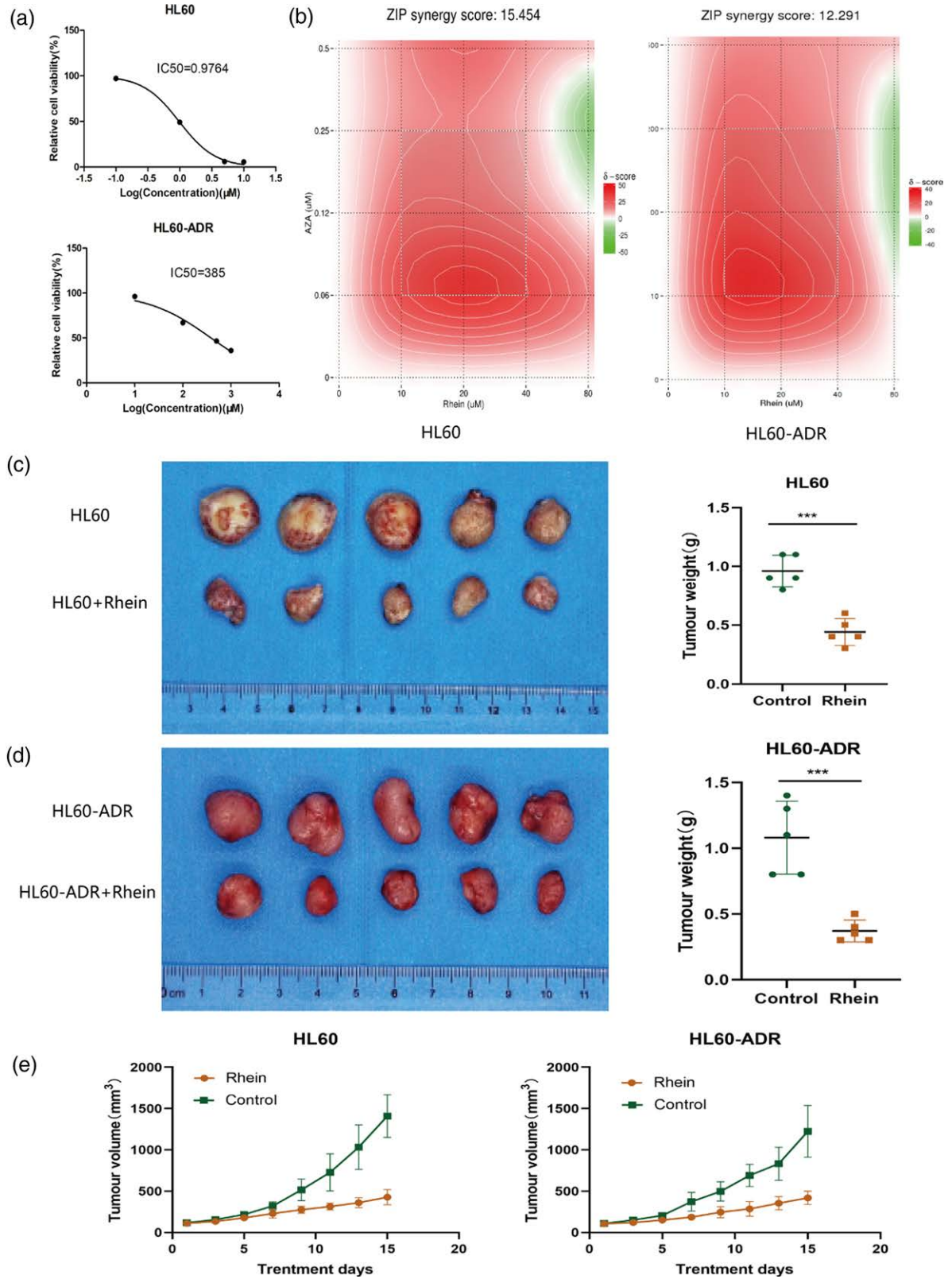

Rhein has synergistic effect with AZA and the anticancer effects on xenograft mouse model: (a) IC50 of AZA on HL60 and HL60-ADR cells after treatment with different concentrations for 48 h. (b) Heatmaps of drug combination responses. Rhein and AZA act synergistically on HL60 and HL60-ADR cells. (c and d) Size and weight of xenograft tumors in rhein group and control group. (e) Volume changes of xenograft tumors in rhein group and control group. ADR, adriamycin; AZA, azacitidine.

ABCB1 in drug-resistant strains. SynergyFinder software ZIP synergy results showed that the average ratio (and maximum value) of antitumor responses caused by drug interactions were 15.45 (21.86) in HL60 and 12.29 (20.67) in HL60-ADR. As depicted in Fig. 4b, the white rectangle represents the area with the largest synergistic effect. Our findings demonstrated that the combination treatment of rhein and AZA synergistically inhibited on the proliferation of both HL60 and HL60-ADR cells. The optimal concentration of rhein when the two drugs worked together was 10 μM, which was the lowest concentration in the area with the strongest synergy. These results demonstrate that even if the concentration of rhein is well below its IC50 value, it can synergistically enhance the cytotoxicity of AZA on AML cells including multidrug resistance AML cells, and can also significantly reduce AZA effective dose in HL60-ADR cells that are resistant to AZA.

Rhein inhibits the growth of transplanted tumors in mice

To further confirm the in-vivo antitumor effect of rhein, we established a xenograft tumor mouse model using HL60 and HL60-ADR and monitored the size of the transplanted tumors. Once the tumor volume reached the predetermined criteria, rhein was injected intraperitoneally into the mice. The mice were sacrificed after 15 days of rhein treatment. The tumors in the rhein group exhibited a significant reduction in size compared to the control group, indicating that rhein effectively inhibited tumor growth.

Discussion

The primary objective of AML treatment is to eradicate minimal residual disease and achieve complete remission. Nonetheless, 10–40% of newly diagnosed patients do not achieve complete remission following chemotherapy. Moreover, even when patients achieve complete remission, approximately 50% will eventually experience AML relapse owing to the development of drug resistance [18]. In clinical practice, upon developing resistance to one drug, a patient may readily acquire resistance to other drugs. Currently, the approach to tackling drug-resistant AML involves either combination therapy or substitution of targeted drugs to enhance treatment outcomes. Our study substantiated the upregulation of FTO expression in patients with newly diagnosed as well as relapsed and refractory AML and demonstrated rhein exerts antitumor effects by inhibiting FTO. More importantly, our findings revealed the favorable efficacy of rhein in AML drug-resistant cells. Notably, rhein was effective not only as a monotherapy but also synergistically enhanced the antitumor effects when combined with AZA to target drug-resistant cells, thereby augmenting the therapeutic effectiveness against AML.

Recent studies have revealed that high FTO expression often leads to increased drug resistance and poor prognosis in tumors, such as oral squamous cell carcinoma and cervical cancer. FTO enhances tumor response to chemotherapy, radiotherapy, and anti-PD1 treatment tolerance by activating the Wnt/β-catenin, NF-κB, and STAT3 signaling pathways [17,19–21]. Moreover, FTO has been shown to augment cell resistance by diminishing m^6A mRNA transcripts [19,22,23]. AML cells overexpressing FTO demonstrate heightened resistance to tyrosine kinase inhibitors (TKIs), while treatment with the FTO inhibitor rhein effectively counteracts this resistance [3].

AML cells with multidrug resistance are characterized by the elevated expression of ABCB1, a member of the ATP-binding cassette transporter transporter family. ABCB1 has a wide range of substrates and can reduce the therapeutic efficacy by actively transporting various drug molecules out of cells [24]. The IC50 values of rhein were found to be similar in both parental AML cells and AML cells with multidrug resistance. This phenomenon may be attributed to the competitive binding of rhein to the active site of FTO, thereby inhibiting the efflux of rhein by ABCB1. Additionally, xenograft tumor mouse models of HL60 and HL60-ADR were established to provide in-vivo evidence of the antitumor efficacy of rhein. Consequently, rhein represents a potential strategy for overcoming multidrug resistance in AML.

Recent research has shown that drug-resistant AML cells 'run fast instead of hiding', indicating that drug resistance is closely related to cell migration [25]. The AKT/mTOR pathway is upregulated in AML, and activation of the mTOR pathway enhances the migratory ability of AML cells [26,27]. Importantly, our study confirmed activation of the mTOR pathway and its involvement in AML drug resistance. Rhein exhibited dose-dependent inhibition of both parental and drug-resistant AML cell migration. Inhibition of the AKT/mTOR pathway by rhein may effectively suppress the migratory potential of AML cells. Additionally, Ren *et al.* demonstrated that rhein exerts inhibitory effects on ovarian cancer cell migration [11].

Elderly patients with AML are characterized by elevated morbidity rates, reduced tolerance to conventional chemotherapy, and a dismal outlook. AZA is frequently administered to elderly patients with relapsed or refractory AML. It exerts its therapeutic effects by disrupting RNA metabolism and inhibiting DNA methylation, which can be enhanced by combination therapy with other drugs [18,28,29]. Yang *et al.* established that rhein in combination with epidermal growth factor receptor (EGFR) inhibitors can increase the sensitivity of pancreatic cancer cells to EGFR inhibitors [12]. Additionally, another study found that rhein and RAD001 exhibit a synergistic effect in gastric cancer [30]. We combined rhein and AZA treatment on HL60 and HL60-ADR

cells, and the results showed a good synergistic effect in both the parental strain and the drug-resistant strain, supporting the potential clinical application of this combination therapy. Utilization of low-dose rhein augments the antitumor efficacy of azacitidine while mitigating drug resistance in AML cells. This finding underscores the potential utility of rhein as a promising therapeutic option for patients who cannot tolerate or develop resistance to conventional treatment regimens.

In conclusion, our study substantiated the upregulation of FTO expression in patients with newly diagnosed as well as relapsed and refractory AML and demonstrated that rhein exerts antitumor effects by inhibiting FTO. Rhein inhibits AML cell proliferation *in vivo* and *in vitro*, inhibits migration of AML cells in a concentration-dependent manner, promotes apoptosis, and inhibits the AKT/mTOR pathway by targeting FTO. Notably, rhein exerts anticancer activity against multidrug-resistance AML cells by specifically binding to the active site of FTO to avoid the pumping effect of ABCB1. Importantly, our study provides the first evidence that combining rhein with AZA results in a synergistic antitumor effect against both parental and drug-resistant strains of AML, ultimately enhancing the therapeutic efficacy of AZA. In light of these findings, rhein represents a promising new treatment option for elderly patients with AML, and it may prove to be a valuable tool for reversing drug resistance in patients with relapsed or refractory AML.

Acknowledgements

This work was supported by the Interdisciplinary Project of the First Hospital of Lanzhou University Ldyyn2020-89 and The Scientific research project of Gansu province drug administration2021GSMPA009.

Conflicts of interest

There are no conflicts of interest.

References

1 Chennamadhavuni A, Lyengar V, Mukkamalla SKR, Shimanovsky A. *Leukemia*. BTI - StatPearls; 2023.
2 Shimony S, Stahl M, Stone RM. Acute myeloid leukemia: 2023 update on diagnosis, risk-stratification, and management. *Am J Hematol* 2023; **98**:502–526.
3 Yan F, Al-Kali A, Zhang Z, Liu J, Pang J, Zhao N, *et al*. A dynamic N^6-methyladenosine methylome regulates intrinsic and acquired resistance to tyrosine kinase inhibitors. *Cell Res* 2018; **28**:1062–1076.
4 Pan Z, Wang B, Hou D, You R, Wang X, Xie W, *et al*. METTL3 mediates bone marrow mesenchymal stem cell adipogenesis to promote chemoresistance in acute myeloid leukaemia. *FEBS Open Bio* 2021; **11**:1659–1672.
5 Li M, Ye J, Xia Y, Li M, Li G, Hu X, *et al*. METTL3 mediates chemoresistance by enhancing AML homing and engraftment via ITGA4. *Leukemia* 2022; **36**:2586–2595.
6 He J, Liu F, Zhang Z. Functions of N^6-methyladenosine in cancer metabolism: from mechanism to targeted therapy. *Biomarker Res* 2023; **11**:40.
7 Mauer J, Luo X, Blanjoie A, Jiao X, Grozhik AV, Patil DP, *et al*. Reversible methylation of m^6A_m in the 5′ cap controls mRNA stability. *Nature* 2016; **541**:371–375.
8 Li Y, Wu K, Quan W, Yu L, Chen S, Cheng C, *et al*. The dynamics of FTO binding and demethylation from the m^6A motifs. *RNA Biol* 2019; **16**:1179–1189.
9 Li Y, Su R, Deng X, Chen Y, Chen J. FTO in cancer: functions, molecular mechanisms, and therapeutic implications. *Trends Cancer* 2022; **8**:598–614.
10 Li Z, Weng H, Su R, Weng X, Zuo Z, Li C, *et al*. FTO plays an oncogenic role in acute myeloid leukemia as a N^6-methyladenosine RNA demethylase. *Cancer Cell* 2017; **31**:127–141.
11 Ren B, Guo W, Tang Y, Zhang J, Xiao N, Zhang L, *et al*. Rhein inhibits the migration of ovarian cancer cells through down-regulation of matrix metalloproteinases. *Biol Pharm Bull* 2019; **42**:568–572.
12 Yang L, Lin S, Kang Y, Xiang Y, Xu L, Li J, *et al*. Rhein sensitizes human pancreatic cancer cells to EGFR inhibitors by inhibiting STAT3 pathway. *J Exp Clin Cancer Res* 2019; **38**:31.
13 You L, Dong X, Yin X, Yang C, Leng X, Wang W, *et al*. Rhein induces cell death in HepaRG cells through cell cycle arrest and apoptotic pathway. *Int J Mol Sci* 2018; **19**:1060.
14 Aittokallio T, Giri AK, Ianevski A. SynergyFinder 2.0: visual analytics of multi-drug combination synergies. *Nucleic Acids Res* 2020; **48**:W488–WW93.
15 Ianevski A, Giri AK, Aittokallio T. SynergyFinder 3.0: an interactive analysis and consensus interpretation of multi-drug synergies across multiple samples. *Nucleic Acids Res* 2022; **50**:W739–W743.
16 Zhang H, Yi J-K, Huang H, Park S, Park S, Kwon W, *et al*. Rhein suppresses colorectal cancer cell growth by inhibiting the mTOR pathway in vitro and in vivo. *Cancers* 2021; **13**:2176.
17 Zhang H, Ma L, Kim E, Yi J, Huang H, Kim H, *et al*. Rhein induces oral cancer cell apoptosis and ROS via suppresse AKT/mTOR signaling pathway in vitro and in vivo. *Int J Mol Sci* 2023; **24**:8507.
18 Thol F, Ganser A. Treatment of relapsed acute myeloid leukemia. *Curr Treat Options Oncol* 2020; **21**:66.
19 Fukumoto T, Zhu H, Nacarelli T, Karakashev S, Fatkhutdinov N, Wu S, *et al*. N^6-Methylation of adenosine of FZD10 mRNA contributes to PARP inhibitor resistance. *Cancer Res* 2019; **79**:2812–2820.
20 Zhou S, Bai ZL, Xia D, Zhao ZJ, Zhao R, Wang YY, *et al*. FTO regulates the chemo-radiotherapy resistance of cervical squamous cell carcinoma (CSCC) by targeting β-catenin through mRNA demethylation. *Mol Carcinog* 2018; **57**:590–597.
21 Yang S, Wei J, Cui Y-H, Park G, Shah P, Deng Y, *et al*. m^6A mRNA demethylase FTO regulates melanoma tumorigenicity and response to anti-PD-1 blockade. *Nat Commun* 2019; **10**:2782.
22 Lin Z, Wan AH, Sun L, Liang H, Niu Y, Deng Y, *et al*. N^6-methyladenosine demethylase FTO enhances chemo-resistance in colorectal cancer through SIVA1-mediated apoptosis. *Mol Ther* 2023; **31**:517–534.
23 Ou B, Liu Y, Gao Z, Xu J, Yan Y, Li Y, *et al*. Senescent neutrophils-derived exosomal piRNA-17560 promotes chemoresistance and EMT of breast cancer via FTO-mediated m6A demethylation. *Cell Death Dis* 2022; **13**:905.
24 Holohan C, Van Schaeybroeck S, Longley DB, Johnston PG. Cancer drug resistance: an evolving paradigm. *Nat Rev Cancer* 2013; **13**:714–726.
25 Hawkins ED, Duarte D, Akinduro O, Khorshed RA, Passaro D, Nowicka M, *et al*. T-cell acute leukaemia exhibits dynamic interactions with bone marrow microenvironments. *Nature* 2016; **538**:518–522.
26 Wang X, Zhong L, Dan W, Chu X, Luo X, Liu C, *et al*. MiR-454-3p promotes apoptosis and autophagy of AML cells by targeting ZEB2 and regulating AKT/mTOR pathway. *Hematology* 2023; **28**:2223874.
27 Rahmani M, Nkwocha J, Hawkins E, Pei X, Parker RE, Kmieciak M, *et al*. Cotargeting BCL-2 and PI3K induces BAX-dependent mitochondrial apoptosis in AML cells. *Cancer Res* 2018; **78**:3075–3086.
28 Müller A, Florek M. 5-Azacytidine/azacitidine. *Recent Results Cancer Res* 2010; **184**:159–170.
29 Thol F, Schlenk RF, Heuser M, Ganser A. How I treat refractory and early relapsed acute myeloid leukemia. *Blood* 2015; **126**:319–327.
30 Gao F, Li R, Wei P-F, Ou L, Li M, Bai Y, *et al*. Synergistic anti-cancer effects of everolimus (RAD001) and rhein on gastric cancer cells via phosphoinositide-3-kinase (PI3K)/protein kinase B (AKT)/mammalian target of rapamycin (mTOR) pathway. *Bioengineered* 2022; **13**:6332–6342.